CANCER EXOSOMES

# AML suppresses hematopoiesis by releasing exosomes that contain microRNAs targeting c-MYB

Noah I. Hornick,[1,2,3]* Ben Doron,[1,2,3]* Sherif Abdelhamed,[1,2,3] Jianya Huan,[1,2,4] Christina A. Harrington,[4,5] Rongkun Shen,[6,7,8] Xiaolu A. Cambronne,[7] Santhosh Chakkaramakkil Verghese,[1,2,3] Peter Kurre[1,2,3,4]†

**Exosomes are paracrine regulators of the tumor microenvironment and contain complex cargo. We previously reported that exosomes released from acute myeloid leukemia (AML) cells can suppress residual hematopoietic stem and progenitor cell (HSPC) function indirectly through stromal reprogramming of niche retention factors. We found that the systemic loss of hematopoietic function is also in part a consequence of AML exosome–directed microRNA (miRNA) trafficking to HSPCs. Exosomes isolated from cultured AML or the plasma from mice bearing AML xenografts exhibited enrichment of miR-150 and miR-155. HSPCs cocultured with either of these exosomes exhibited impaired clonogenicity, through the miR-150– and miR-155–mediated suppression of the translation of transcripts encoding c-MYB, a transcription factor involved in HSPC differentiation and proliferation. To discover additional miRNA targets, we captured miR-155 and its target transcripts by coimmunoprecipitation with an attenuated RNA-induced silencing complex (RISC)–trap, followed by high-throughput sequencing. This approach identified known and previously unknown miR-155 target transcripts. Integration of the miR-155 targets with information from the protein interaction database STRING revealed proteins indirectly affected by AML exosome–derived miRNA. Our findings indicate a direct effect of AML exosomes on HSPCs that, through a stroma-independent mechanism, compromises hematopoiesis. Furthermore, combining miRNA target data with protein-protein interaction data may be a broadly applicable strategy to define the effects of exosome-mediated trafficking of regulatory molecules within the tumor microenvironment.**

## INTRODUCTION

Acute myeloid leukemia (AML) is the most common acute leukemia in adults; its collateral suppression of normal hematopoiesis leads to anemia, neutropenia, and thrombocytopenia (*1*). This has traditionally been ascribed to successive marrow infiltration by leukemic blasts and resultant overcrowding (*2*), an explanation that fails to address the occurrence of cytopenias in patients with normal marrow cellularity or, more rarely, in those with exclusively extramedullary AML. Studies show that leukemic invasion causes extensive remodeling of the marrow microenvironment (*3*, *4*) and thereby indirectly interferes with residual hematopoietic stem and progenitor cell (HSPC) function (*5*, *6*). Thus, the aggregate clinical and experimental observations suggest active regulation, but the specific mechanisms are as yet elusive.

Exosomes—nanoscale, membrane-enclosed extracellular vesicles—mediate the functional transfer of protein, messenger RNA (mRNA), and microRNA (miRNA) between cells (*7*, *8*). Work in our laboratory and those of others have demonstrated that AML cells secrete extracellular vesicles that conform to the definition of exosomes and transfer RNA to multiple cell types within the bone marrow microenvironment. Additionally, whereas the secretion of exosomes is a constitutive homeostatic process, we previously showed that exposure of HSPC to exosomes derived from primary AML blasts or AML cell lines, but not those from normal $CD34^+$ cell cultures, phenocopies the suppression of colony-forming capacity in animals bearing an AML xenograft (*5*, *6*). Given their selective enrichment in vesicles, exosomal transfer of specific miRNA and translational suppression of mRNA targets represent another plausible explanation for the leukemia-associated loss of HSPC function.

Here, we investigated the molecular mechanism underlying AML exosome–driven systemic suppression of hematopoiesis. Through systematic analysis of exosomal miRNA content, we found that leukemic transformation altered the miRNA profile of exosomes and that delivery of highly abundant exosomal miRNA, specifically miR-150 and miR-155, was sufficient to suppress HSPC clonogenicity. Candidate- and discovery-based strategies revealed the regulatory networks targeted by AML exosome trafficking. Together, our study provides both insight into a major mechanism of disease morbidity and an experimental workflow for the future study of vesicle miRNA action in diverse recipient cell populations.

## RESULTS

### Leukemia-derived exosomes are sufficient to induce systemic impairment of hematopoiesis

We and others previously validated the human Molm-14 cell line as a highly reproducible experimental model for high-risk (FLT-3 $ITD^+$) AML

[1]Department of Pediatrics, Oregon Health & Science University, Portland, OR 97239, USA. [2]Pediatric Cancer Biology, Oregon Health & Science University, Portland, OR 97239, USA. [3]Papé Family Pediatric Research Institute, Oregon Health & Science University, Portland, OR 97239, USA. [4]Knight Cancer Institute, Oregon Health & Science University, Portland, OR 97239, USA. [5]Integrated Genomics Laboratory, Oregon Health & Science University, Portland, OR 97239, USA. [6]Department of Biology, State University of New York, Brockport, NY 14420, USA. [7]Vollum Institute, Oregon Health & Science University, Portland, OR 97239, USA. [8]The College at Brockport, State University of New York, Brockport, NY 14420, USA.
*These authors contributed equally to this work.
†Corresponding author. Email: kurrepe@ohsu.edu

(*8*). To accurately track the leukemic burden in mice, we transduced Molm-14 cells with a lentivirus expression vector containing firefly luciferase (luc), as previously described (*9*). Serial in vivo imaging of luciferase expression provided a quantitative measure of Molm-14 burden in immunocompromised NSG [nonobese diabetic/severe combined immunodeficient/interleukin (IL)–2 receptor γ–null] mice (Fig. 1A). Chimerism analysis of bone marrow at sacrifice showed consistent endpoint correlation between *hsa*-CD45 expression and the luminescence data, supporting this method for observing the highly reproducible disease kinetics (fig. S1). To determine the trafficking of exosomes in this in vivo model, we chose a genetic labeling method, whereby cells stably express a myristoylated reporter gene (*10*). By design, the myristoyl motif expressed at the N termini of fluorophore leads to quantitative incorporation into the lipid membrane structure of the Molm-14 cells and secreted vesicles. Exosomes derived from Molm-14 cells containing this transgene provide bright fluorescence signal, enabling one to monitor the trafficking of vesicles both in vitro and in vivo. As proof of principle, we imaged exosomes harvested from the Molm-14 line harboring myristoylated Tomato (mTomato) (Fig. 1B). For our in vivo studies, we used myristoylated green fluorescent protein (mGFP) for its compatibility with our fluorescent antibodies used for flow cytometry. Confocal imaging of purified murine c-KIT$^+$, SCA-1$^+$, LIN$^-$ HSPC from xenografts revealed GFP$^+$ vesicles in their cytosol, thus demonstrating the trafficking of leukemic vesicles to the HSPC (Fig. 1C). To further demonstrate the systemic nature of exosome signaling, we obtained serum from mice xenografted with either Molm-14 or HL-60 (a leukemic cell line also previously validated for exosome release and HSPC suppression) for exposure to murine c-KIT$^+$ HSPC (*6*). This in vitro exposure to serum from mice bearing AML xenografts significantly reduced the clonogenicity of c-KIT$^+$ HSPC in colony-forming assays. To determine the specific contribution of exosomes as mediators of this phenotype, we replicated the exposure of c-KIT$^+$ cells to exosomes purified from the serum of mice bearing Molm-14 xenografts, again observing a similar loss in clonogenicity (Fig. 1D). Finally, we performed both intravenous and contralateral intrafemoral injections with purified serum exosomes from control and Molm-14 xenografts into naïve NSG mice. c-KIT$^+$ cells were harvested from each femur 48 hours after injection,

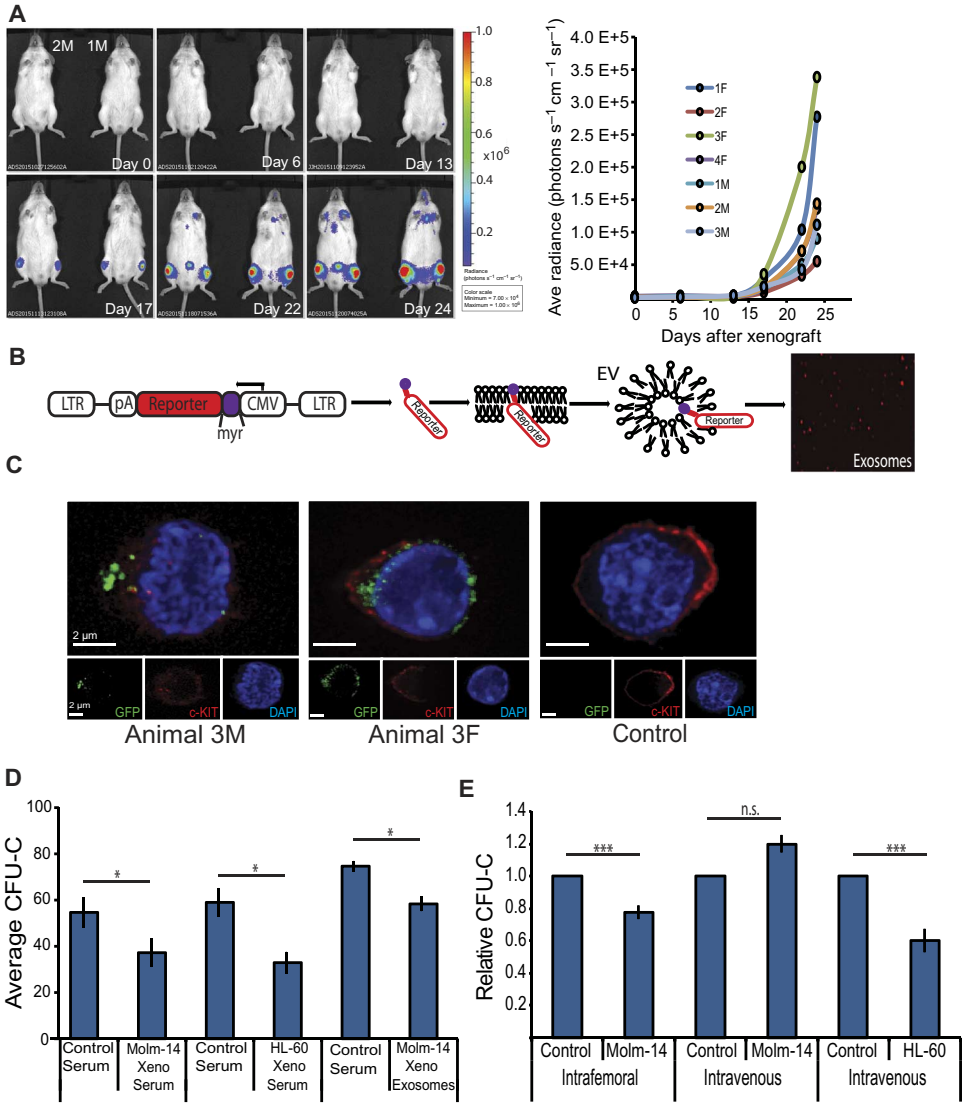


**Fig. 1. Leukemia systemically impairs HSPC function.** (**A**) Engraftment of *luc*$^+$ Molm-14 cells was tracked and quantified using in vivo imaging. Two representative mice (1M and 2M, left and right) were imaged at multiple time points after engraftment. Days 0, 6, 13, 17, 22, and 24 are shown. Engraftment was quantitated by radiance as photons s$^{-1}$ cm$^{-2}$ sr$^{-1}$;. 1M and 2M are individual animal designations. (**B**) Schematic of mGFP incorporation into the cell membrane. Exosomes harvested from Molm-14 cells transduced with a lentiviral vector containing the mGFP expression cassette were mGFP$^+$ (representative image, right). LTR, long terminal repeat; pA, poly-adenylate; CMV, cytomegalovirus; EV, extracellular vesicle. (**C**) Confocal microscopy for GFP$^+$ vesicles in the cytosol of HSPC from mice engrafted with *mGFP*$^+$ Molm-14. Bone marrow aspirates from control and xenografted mice were sorted for c-KIT$^+$, SCA-1$^+$, and LIN$^-$ markers. Scale bars, 2 μm. DAPI, 4′,6-diamidino-2-phenylindole. (**D**) c-KIT$^+$ HSPCs from C57BL/6 mice were exposed to serum or serum exosomes collected from healthy (Control) and xenografted (Xeno) mice and then plated in methylcellulose and assessed for clonogenicity. CFU-C, CFU in culture. (**E**) Clonogenicity of c-KIT$^+$ cells harvested from NSG mice 48 hours after mice were injected as indicated with serum exosomes from mice bearing xenografts. Data are expressed relative to mice injected with control serum. Data are means ± SEM of a representative of cells derived from at least three mice and plated in triplicate (*$P$ < 0.05; ***$P$ < 0.001; n.s., not significant, by Student's $t$ test).

and a significant decrease in clonogenicity was observed in HSPC from the Molm-14 exosome–injected femur. Notably, this phenotype was not observed in mice receiving a one-time intravenous injection of exosomes, presumably due to the reduced dose of exosomes reaching HSPC within the marrow when delivered systemically. However, we previously demonstrated the comparatively more pronounced impact of HL-60 exosomes on HSPCs in vitro and in vivo, even during minimal marrow invasion (*6*), suggesting that cell source and a larger cumulative exposure to exosomes might be sufficient to affect marrow suppression. Results herein support this notion, revealing significant suppression of HSPC clonogenicity after two intravenous injections of serum exosomes from an HL-60 xenograft (Fig. 1E). This observation is further strengthened by the coincident loss of expression of several transcripts including *c-Myb*, *c-Kit*, and *Dnmt1* in c-KIT$^+$ cells harvested from these exposures (figs. S2 and S3), as shown previously (*6*). Combined, these in vitro and in vivo serum and serum-exosome transfer experiments underscore the systemic nature of vesicle trafficking beyond the immediate tissue compartment.

## Leukemia exosomes exert dose-dependent effects and contain selected predominantly mature miRNA

To address the hypothesis that direct exosome delivery of miRNA contributes to the reduction in the colony-forming capacity of murine HSPC, we examined the relationship between exosome dose and suppression of clonogenicity. We exposed murine HSPC to exosome dilutions prepared from HL-60 cultures. After 48 hours of exposure, we found that colony counts inversely correlated with the exosome dose (Fig. 2A). Furthermore, the relative abundance of hematopoietic transcripts also correlated with the amount of exosomes (Fig. 2B). Together, these observations suggested that quantitatively transferred miRNA may be responsible for regulating hematopoietic transcripts and, consequently, for suppression of clonogenicity. To test this hypothesis, we undertook a global comparison of the miRNA contained within the AML cell lines HL-60 and Molm-14, and within the exosomes secreted by these cells, alongside cultures of nonmalignant cord blood–derived CD34$^+$ cells and their exosomes. An miRNA microarray evaluation of these samples revealed clear distinctions between both cells and exosomes as well as between malignant and nonmalignant exosomes (Fig. 2C), a position further strengthened by principal components analysis (Fig. 2D). These data suggest active enrichment and exclusion of specific transcripts into exosomes and demonstrate unique differences between leukemic and nonleukemic cell-derived exosome miRNA profiles. Comparing array probes for mature miRNA to those for less-processed pre-miRNA revealed that the vast majority of the miRNA trafficked within exosomes is mature and could function inside a recipient cell without further processing (Fig. 2E). We therefore turned our attention to the cellular targets of miRNA enriched in leukemic exosomes to identify potential candidates responsible for the observed loss of clonogenicity.

## Exosome-delivered miRNAs down-regulate critical hematopoietic regulators, including c-MYB

We focused on miR-155 because of its overrepresentation in leukemic exosomes (*11*) along with the relevance of its targets *Cebp*β, *Tab2* (*12*, *13*), and *c-Myb* in particular. The transcription factor c-MYB influences hematopoietic differentiation (*14*) and stem cell mobilization (*15*), whereby *c-Myb*$^{-/-}$ mice exhibit hematopoietic impairment strikingly similar to that observed in our exosome-treated HSPC (*14*). A search for other miRNA targeting *c-Myb* led us to explore miR-150 (*16*), another highly abundant miRNA within both Molm-14 and HL-60 exosomes (*11*). qRT-PCR evaluation of murine HSPC revealed a substantial increase in miR-155 abundance after exposure to AML-derived exosomes (Fig. 3A), consistent with the transfer of exogenous miRNA to recipient cells. Serum exosomes harvested from xenografts showed a substantial increase in miR-155 when compared to serum exosomes of control mice (Fig. 3B). Using a dual-luciferase reporter system, we verified the targeting of our genes of interest by miR-155, including both human and murine *c-Myb* 3′ untranslated regions (3′UTRs). We also validated that miR-150 targets the murine *c-Myb* transcript, whereas the *Caenorhabditis elegans*–derived miR-67 (cel-miR-67) negative control did not target any murine 3′UTR (Fig. 3C). The miRNA-mediated suppression of *c-Myb* was replicated using exosomes in place of transfection of miR-155 mimic (Fig. 3D). This work provides the first direct evidence of *c-Myb* suppression by exosome-delivered miRNA.

## Suppression of c-Myb by exosomal miR-155 compromises HSPC clonogenicity

We used an RNA interference strategy to demonstrate that translational *c-Myb* suppression is sufficient to impair clonogenicity in murine HSPC. *c-Myb*–targeting small interfering RNAs (siRNAs) were electroporated into c-KIT$^+$ cells, incubated for 48 hours, and then assayed for colony-forming capacity. This experiment revealed a significant deficit in the *c-Myb*–suppressed cells compared to control siRNA–electroporated cells and implicitly controlled for the anticipated effect of electroporation on colony formation (Fig. 4A). qRT-PCR showed more than a 10-fold reduction in *c-Myb* transcript abundance in the siRNA-treated conditions compared to the siRNA control (normalized to *Gapdh*) (Fig. 4B). To demonstrate the contribution of exosomal miR-155 to this effect in the exosome exposure paradigm, we electroporated synthetic anti-miRNA oligonucleotides (*17*) into murine HSPC to protect them from exogenous delivery of miRNA via HL-60 exosomes. Electroporated cells were incubated with either vehicle or HL-60 exosomes for 48 hours before colony-forming unit (CFU) plating. Cells transfected with anti–miR-155 demonstrated partial protection against loss of clonogenicity compared to cells containing the control anti-miRNA. We then electroporated both anti–miR-155 and anti–miR-150 into HSPC, which yielded complete protection against the effects of exposure to HL-60 exosomes (Fig. 4C). *c-Myb* transcript abundance was assayed by qRT-PCR at the time of CFU plating and correlated with the rescue of clonogenicity (Fig. 4D). To address the possibility that the experimental transfection of anti-miRs itself may act on the endogenous miRNA within HSPC, we transduced the HL-60 cell line with a lentivirus construct that constitutively expresses a short hairpin RNA (shRNA) against miR-155(*16*). This miR-155 knockdown line provided a source of leukemic exosomes specifically deficient in this miRNA to isolate its unique contribution to total exosome effect. As anticipated, this modified cell line exhibited marked decrease in detectable miR-155 in both cell lysates and exosomes (Fig. 4E). The knockdown of miR-155 had no effect on cell growth or the size distribution of exosomes (figs. S4 and S5). We compared the hematopoietic potential of c-KIT$^+$ cells exposed to exosomes from this line relative to exosomes harvested from wild-type HL-60. The miR-155 knockdown line exosomes did not confer the clonogenic suppression observed in wild-type HL-60 exosomes (Fig. 4F). These experiments demonstrate that exosomes enriched with a select set of miRNA, specifically miR-155 and miR-150, can contribute to impaired HSPC function. Consistent with studies in *c-Myb* knockout animals, the translational suppression of *c-Myb* by HL-60 exosomes via trafficking of highly abundant miRNA is sufficient to suppress murine HSPC clonogenicity.

## Leukemia exosomes contain miRNAs that target key hematopoietic regulatory networks

Although the specific action of miR-150 or miR-155 on *c-Myb* contributes to HSPC suppression, exosomes deliver highly complex cargo

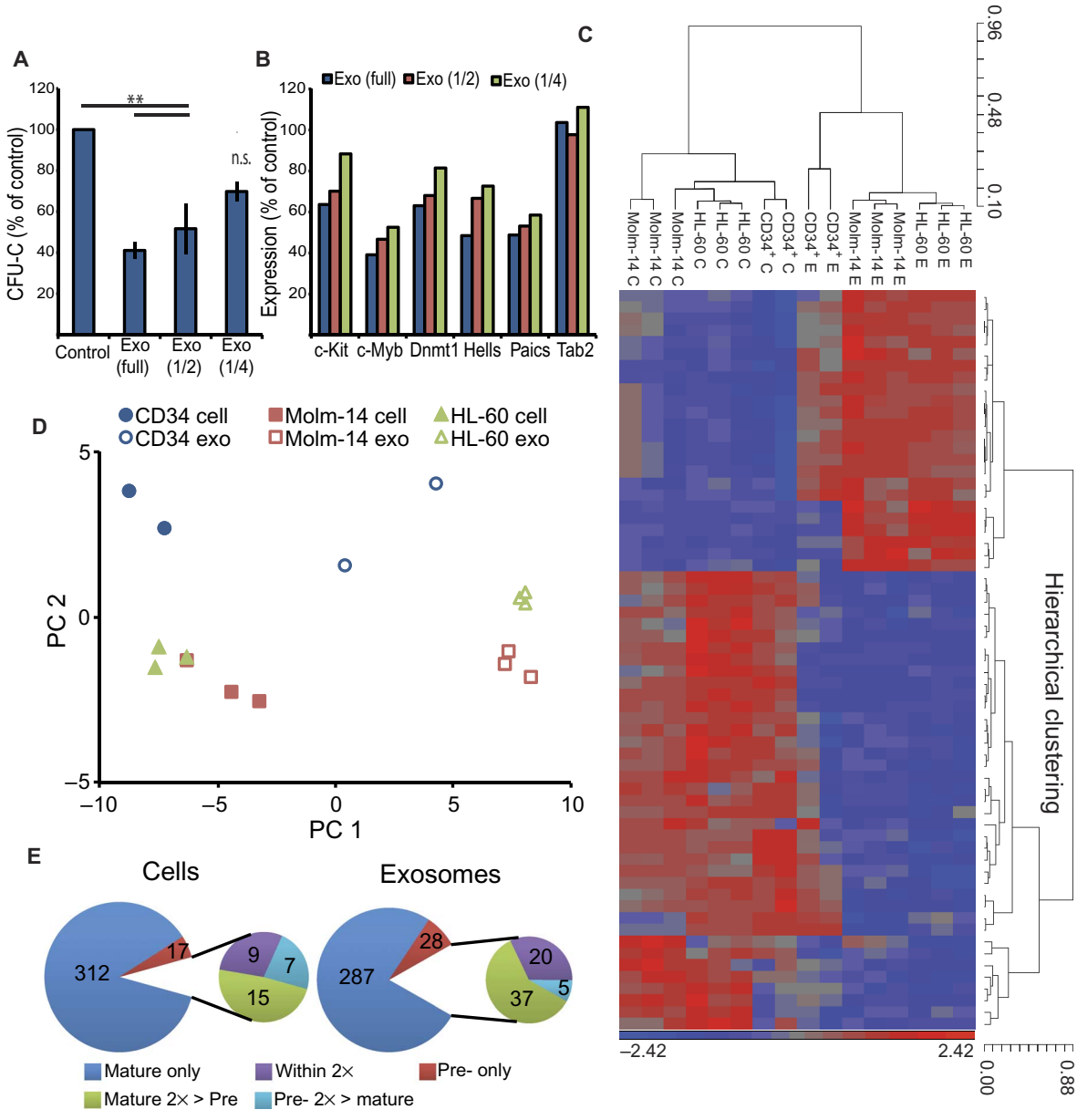


**Fig. 2. Leukemia exosomes suppress HSPC function and are enriched with specific miRNA transcripts.** (**A**) Colony-forming capacity in murine c-KIT$^+$ cells cultured with three doses of HL-60–derived exosomes for 48 hours and plated in methylcellulose. Data are means ± SEM of a representative of cells derived from at least three mice, plated in triplicate (*$P < 0.05$; **$P < 0.01$; ***$P < 0.001$; n.s., not significant, by Student's $t$ test). (**B**) Expression of hematopoietic and epigenetic regulatory genes measured by quantitative reverse transcription polymerase chain reaction (qRT-PCR) in c-KIT$^+$ cells exposed to three doses of HL-60–derived exosomes (Exo). Expression was normalized to glyceraldehyde-3-phosphate dehydrogenase (GAPDH) and presented relative to expression in unexposed c-KIT$^+$ cells. (**C**) Microarray comparison of miRNA isolated from Molm-14, HL-60, and nonmalignant human CD34$^+$ cells ("C") and respective exosomes ("E"). Targets with more than twofold mean difference between producing cell and exosome are shown, robust multiarray average (RMA)–corrected, and standardized to a mean of 0 and an SD of 1. Dendrogram values are 1 – Pearson's R. (**D**) Principal components (PC) analysis, performed after gene selection for all (63) targets detected in all samples and demonstrating significant [false discovery rate (FDR) < 0.05] enrichment in leukemic exosomes relative to those from cells. (**E**) Comparison and categorization (as measured by microarray) of mature and pre-miRNA (Pre) abundance in Molm-14 cells and exosomes as detected by microarray.

to recipient cells, and evaluating their effect in a reductionist approach risks missing the bigger picture. We therefore began a global evaluation of the targets of exosomal miRNA with an assay into the target set of miR-155. For these experiments, we chose the RNA-induced silencing complex (RISC)–trap approach for its ability to provide an unbiased target set based on active binding of mRNA by miR-155–loaded RISC complexes (*18*). Using RISC-trap, we identified miRNA targets by immunoprecipitating a dominant negative RISC loaded with the miRNA of interest, extracting

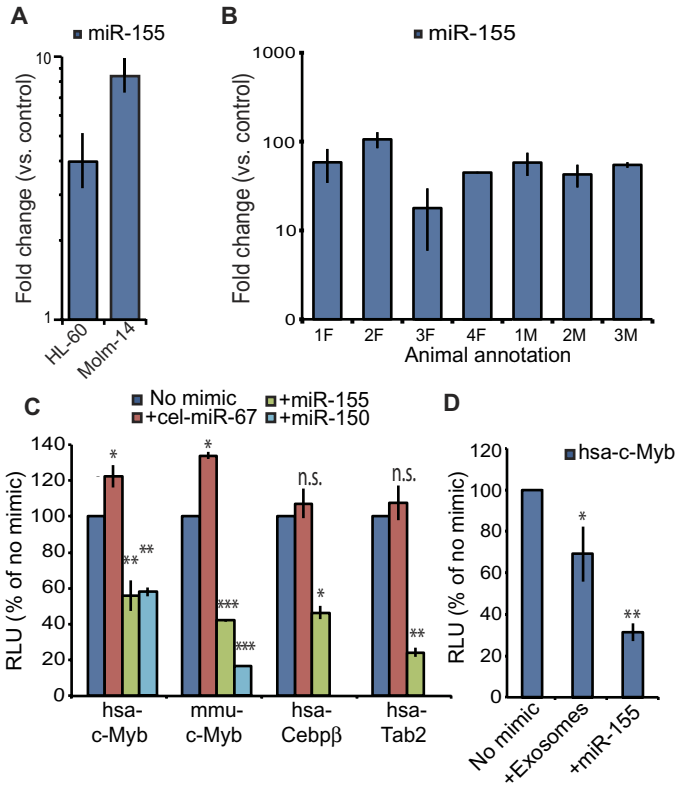


Fig. 3. Exosome-delivered miR-155 down-regulates recipient cell abundance of c-Myb. (**A**) Fold change in miR-155 abundance by qRT-PCR in c-KIT$^+$ cells cultured overnight with HL-60– or Molm-14–derived exosomes relative to controls. *U6 small nuclear RNA* (*snRNA*) was the reference gene. (**B**) Fold change in abundance of miR-155 in exosomes from the serum of xenografted mice relative to that from two control mice as assessed by qRT-PCR. 1F, 2F, etc., designate individual animal. (**C**) 3′UTRs of candidate targets were cloned into the psiCheck-2 vector, and miRNA targeting was determined by loss of luminescence when coexpressed with miRNA of interest, compared to coexpression with control miRNA or vehicle. Data are % RLU (relative luciferase units) of the no-miRNA control. (**D**) *c-Myb* 3′UTR luciferase assay was performed as in (C) with the exception that luminescence was read 24 hours after transfection, using HL-60–derived exosomes alongside miR-155 mimic. Data are means ± SEM from at least three independent experiments, performed in technical triplicates (*$P$ < 0.05; **$P$ < 0.01; ***$P$ < 0.001; n.s., not significant, by Student's $t$ test).

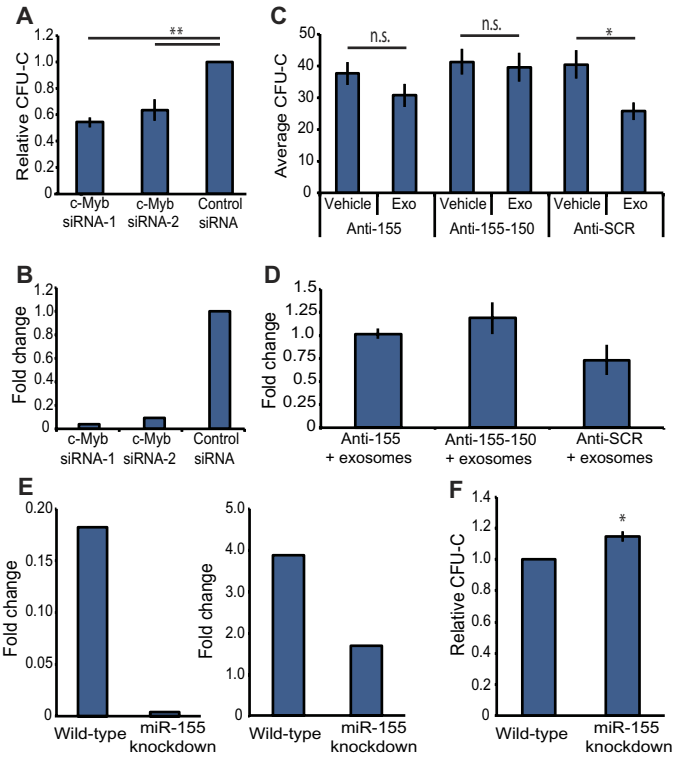


Fig. 4. c-Myb suppression by exosomal miR-155 compromises HSPC clonogenicity. (**A**) Clonogenicity of murine c-KIT$^+$ cells transfected with siRNA targeting *c-Myb* or control. (**B**) qRT-PCR quantification of *c-Myb* RNA in c-KIT$^+$ cell lysates 48 hours after siRNA transfection. (**C**) Clonogenicity in c-KIT$^+$ cells transfected with anti–miR-155, anti–miR-155 and anti–miR-150, or anti–miR-scramble (SCR) and then exposed to either HL-60–derived exosomes or vehicle. (**D**) qRT-PCR analysis of RNA extracted from cells described in (C). (**E**) qRT-PCR for the abundance of miR-155 wild-type and miR-155 knockdown HL-60 cells and from their purified exosomes. *U6 snRNA* was the reference gene. Data are fold change relative to wild-type. (**F**) Clonogenicity of c-KIT$^+$ cells exposed to exosomes derived from wild-type HL-60 or miR-155 knockdown HL-60. Data are means ± SEM of a representative of cells derived from at least three mice and plated in triplicate (*$P$ < 0.05; **$P$ < 0.01; n.s., not significant, by Student's $t$ test).

and sequencing the complexed mRNA, and comparing results to those obtained using two distinct miRNA. Transcripts significantly enriched in the samples derived from cells transfected with the miRNA of interest are identified through statistical analysis. For this study, we compared miR-155 targets against miR-132 and miR-137 targets. Targets enriched from the miR-155 RISC-trap data were compared to the lists of in silico predicted targets available through miRWalk (Fig. 5A) (*19*). The RISC-trap results contained transcripts previously verified as miR-155 targets [including *Bach1*, *Cebp*β, and *Tab2* (*13*)], those predicted by miRWalk (including *Abi2* and *Tet1*), and those neither verified nor predicted (such as *Chek2*, *Chordc1*, *Nbea1*, and *Znf431*), which we validated with the dual-luciferase assay (Fig. 5B). Intrigued by the broad regulatory potential of many of these targets, we created an overview of the different interconnected pathways that AML exosome–contained miR-155 could be expected to affect. To accomplish this, we chose the STRING protein interaction database as a central repository of information about regulatory networks (*20*). Using the most enriched mRNA detected in the miR-155 data set as input (greater than 2× enrichment when compared to miR-132 and miR-137 targets) (table S1), we collected the set of interactions contained within STRING that involved these proteins. With Cytoscape software (*21*), the data set was filtered for experimentally validated interactions of human proteins and nodes with only one interaction were removed. This revealed a central network of proteins directly regulated by miR-155 and the interacting partners of those proteins (Fig. 5C). Together, our analysis yielded compelling insights regarding the activity of miR-155. In addition to its numerous well-studied direct targets, miR-155 appears to indirectly manipulate the actions of several proteins with established roles in malignancy [TP53, BRCA1, and MYC (*22*–*24*)] and hematopoiesis [CTNNB1, RUNX1, and MLL (*25*–*27*)]. For proof of

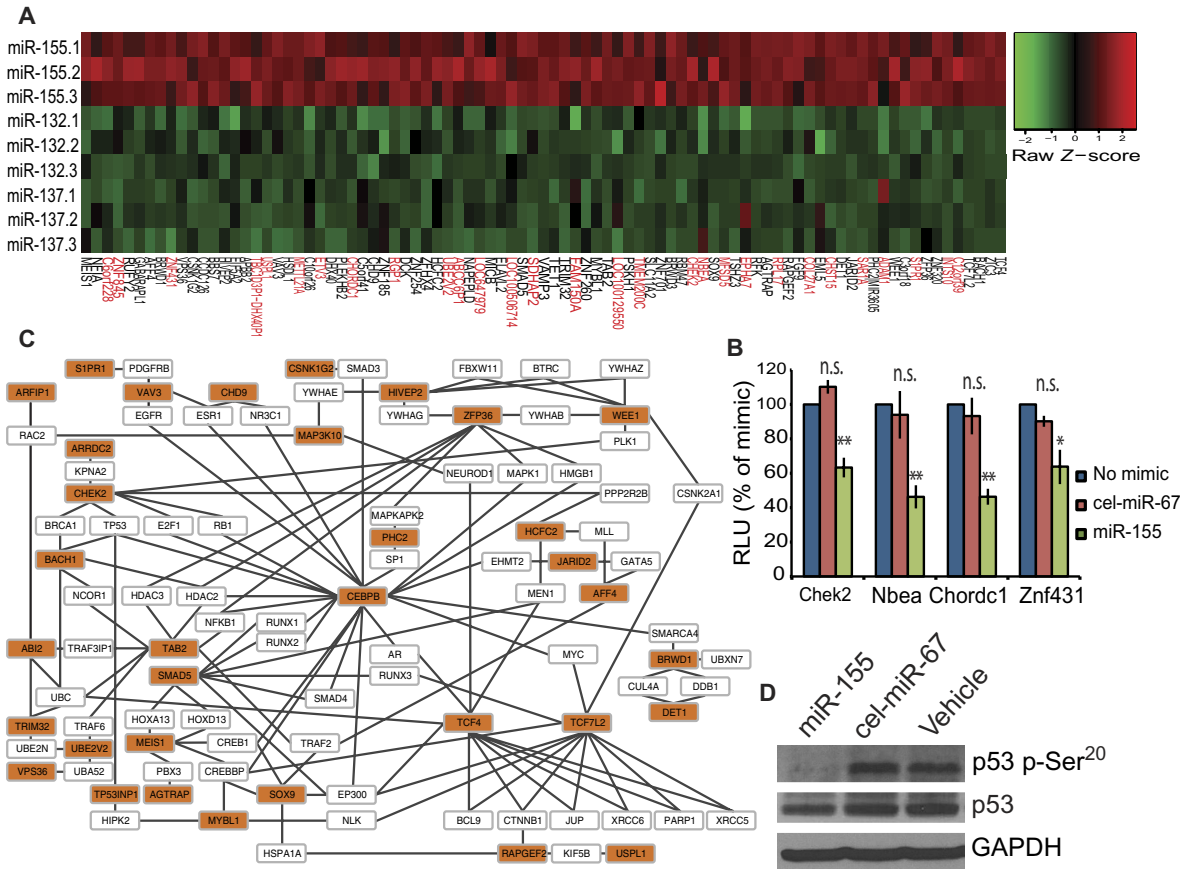


Fig. 5. Exosome miRNA target networks overlap at key hematopoietic regulators. (A) Predicted targets of miR-155 identified by RISC-trap in HEK293T cells, compared with those of miR-132 and miR-137 as controls. Targets in red were not predicted by miRWalk, using the DIANA-mT, miRanda, miRDB, miRWalk, RNA22, and TargetScan in silico prediction algorithms. (B) Targets from the miR-155 RISC-trap data set were validated with the dual-luciferase assay described in Fig. 3C. Data are means ± SEM from at least three independent experiments, performed in technical triplicates (*$P < 0.05$; **$P < 0.01$; n.s., not significant, by Student's *t* test). (C) Interacting partners of miR-155 targets identified by STRING database, using the targets in (A) as input queries. Results were filtered by species and interaction detection method, leaf nodes were removed, and the remaining connected nodes were color-coded. (D) Western blots against phosphorylated Ser$^{20}$ of p53, p53, and GAPDH in lysates from HEK293T cells 48 hours after transfection with miR-155, cel-miR-67, or vehicle. Blots are representative of three experiments.

principle, we demonstrated the indirect effect of exogenous miR-155 activity by analyzing the phosphorylation of p53 in human embryonic kidney (HEK) 293T cells transfected with miR-155, cel-miR-67, or vehicle. Checkpoint kinase 2 (CHEK2) activates p53 (*28*); thus, a miR-155–mediated decrease of CHEK2 should reduce the phosphorylation of p53 on Ser$^{20}$. Exogenous introduction of miR-155 reduces p53 phosphorylation at this residue (Fig. 5D). Together, these data demonstrate the dynamic activity of miRNA trafficking and its influence on both direct and indirect targets in recipient cells.

## DISCUSSION

The failure of the residual HSPC pool to meet the demand for adequate blood cell production creates substantial morbidity for patients with AML. Although a compelling explanation for the characteristic erosion of hematopoiesis had long remained elusive, several recent studies indicate that residual HSPC function is indirectly suppressed, in a process involving altered stromal support (*3*–*6*). Our previous work suggests an additional direct crosstalk between AML cells and the HSPC compartment via exosomes, and indicates the selective exosome enrichment of miRNA (*6*, *11*, *29*) as an additional candidate mechanism for the observed HSPC suppression in the leukemic microenvironment (*3*, *30*–*32*). Here, we confirmed the exosome-based HSPC suppression in vitro and in vivo, its transferability from xenografted to naïve animals via serum exosomes, and the specific action of highly abundant miRNA on a critical transcription factor.

Our initial microarray investigation demonstrated that both leukemogenesis and exosome production exert marked selection bias on miRNA composition. Consistent with a report that exosomes contain elements of the miRNA processing machinery (*33*), miRNA contained within exosomes were found to be predominantly fully processed, with a minority representation of pre-miRNA. We began a more mechanistic investigation with emphasis on the leukemia- and exosome-enriched miR-155, because it has established relevance in both hematopoiesis and leukemia (*23*). Several groups have shown that the transcription factor *c-Myb* is a direct target of miR-155, and we found that translational suppression of *c-Myb* by AML exosome–contained miR-155 or by synthetic miR-155 mimics conferred phenotypic changes that were consistent with those seen in genetic loss-of-function studies (*34*). Although miR-155 was sufficient to impair

clonogenicity in exosome-treated HSPC, full protection from this effect was only conferred when both exosome-carried suppressors of *c-Myb*, miR-150 and miR-155, were blocked by transfection of synthetic anti-miR sequences. We then used shRNA to suppress the expression of miR-155 in the producing cells and thereby limit its incorporation in exosomes. In accordance with our other data, exosomes depleted of miR-155 exhibited an impaired capacity to suppress clonogenicity of HSPC. Although it is unlikely that exosomal suppression of *c-Myb* accounts entirely for impaired hematopoiesis, these experiments provide the first illustration of a mechanism for the direct suppression of hematopoiesis resulting from miRNA trafficking by leukemic exosomes. Although we previously showed that $CD34^+$ cell culture–derived exosomes do not confer HSPC suppressive effects in xenografts (*6*), it remains unclear what influence these exosomes may have on healthy HSPCs. It is conceivable that the loss of physiologic HSPC vesicle trafficking that occurs during leukemogenesis alongside the introduction of leukemic exosomes exerts similarly powerful effects. More broadly, the contributions exosome signaling makes to physiologic bone marrow function await future study. Moreover, the experiments described herein provide support for a model in which AML exerts systemic control over hematopoiesis through trafficking of select miRNA in extracellular vesicles.

As a discovery tool for targets not currently predicted by existing databases, RISC-trap captures the interactions of miRNAs with endogenous target host cell transcripts, an experimental approach ideally suited to dissect the overall impact of leukemic exosomal miRNA in the marrow microenvironment. Here, analysis of the global miR-155 transcript target set produced several novel targets with regulatory potential that were not bioinformatically predicted (*28*, *35*). These data sets, when further combined with interaction data from STRING, created a model that reflects the overall impact of a transferred miRNA on the recipient cell. The network presented in Fig. 5B represents one such interaction model and illustrates the potential regulatory complexity of exogenous miRNA trafficking. To improve robustness during discovery and network analysis, we used an enrichment cutoff of 2× to create a heat map of the most enriched miR-155 targets. Consistent with our functional studies and validating the overall strategy, *c-Myb* was significantly overrepresented in our RISC-trap data set when compared to miR-132 and miR-137 (1.86× and 1.72×, respectively) while not meeting the 2× cutoff for inclusion in our downstream analyses (table S1). Thus, our bioinformatics approach complements the RISC-trap as a discovery tool and provides a broadened perspective to illustrate how pivotal oncogenes, tumor suppressors, and transcription factors can become indirect targets via their interacting partner proteins. Conceptually, combining this information with transcriptome analysis of the different cell types present in the bone marrow enables the development of predictive algorithms to dissect cell-cell signaling events.

In summary, our data indicate a direct crosstalk between leukemic and residual hematopoietic cells in the bone marrow, specifically by exosomal miRNA trafficking between cells. These observations extend our understanding of the coordinate suppression of HSPC during leukemic adaptation of the marrow. Conceivably, the unique miRNA profile of AML exosomes has the potential to increase leukemic fitness by dysregulating other cell types in the bone marrow. The tools described herein can be readily adapted to the systematic analysis of exosomal miRNA targeting other niche cell populations, as well as the study of exosomal trafficking in other tumor types.

## METHODS

### Cell culture and exosome preparation

HL-60 and Molm-14 cells were obtained from the laboratory of J. Tyner and were cultured in RPMI (Gibco) with 10% fetal bovine serum (FBS) (GemCell) and 1× penicillin/streptomycin (Gibco) at 37°C, 5% $CO_2$, and >95% humidity. Human $CD34^+$ cord blood progenitors (New York Blood Center) were enriched by MACS cell separation (Miltenyi Biotec) and cultured in serum-free medium (STEMCELL Technologies) supplemented with penicillin/streptomycin (100 U/ml), FMS-like tyrosine kinase 3 ligand (40 ng/ml), stem cell factor (SCF) (25 ng/ml), and thrombopoietin (50 ng/ml) (Miltenyi Biotec). Exosomes were isolated by differential centrifugation as described previously (*29*). AML cells were cultured for 48 hours, the culture medium was spun at 300*g* for 10 min to remove cells, and then the supernatant was spun at 2000*g* for 20 min and at 10,000*g* for 20 min to remove cellular debris. The supernatant was centrifuged at 100,000*g* for 2 hours. Exosomes were either resuspended in phosphate-buffered saline (PBS) or used for RNA extraction. RNA was extracted from exosomes or cells using RNeasy or miRNeasy kits (Qiagen) according to the manufacturer's instructions. The exosome miRNA content from xenografts and control animals was determined after exosome isolation from serum using ExoQuick (System Biosciences), an approach validated by others.

### Exosome visualization

To visualize exosomes, we stably transduced Molm-14 cells to express either mGFP (for xenografts) or mTomato (for purified exosomes). Primary murine HSPCs were harvested from either control or Molm-14–mGFP xenografted NSG mice. LIN-depleted bone marrow cells were washed twice in PBS and labeled with allophycocyanin-conjugated anti–c-KIT (Life Technologies) antibodies. Slides were mounted with Fluoromount-G (SouthernBiotech). Microscopy was performed on an Olympus IX71 with a 60× 1.4 numerical aperture oil lens. *Z*-stacks were acquired every 0.2 μm with a *Z*-stack center bright-field reference, and images were processed with DeltaVision SoftWoRx Explorer.

### Mice and xenografts

NSG mice were purchased from The Jackson Laboratory. Animals 6 to 8 weeks old were used in the experiments. Molm-14 or human cord blood–derived $CD34^+$ cells ($1 \times 10^5$ per animal) or HL-60 cells ($5 \times 10^6$ per animal) were engrafted into nonirradiated animals by tail vein injection. Chimerism was determined by In Vivo Imaging System using leukemia-bearing *Luciferase* or by flow cytometry on peripheral blood using a human CD45 antibody. Animals were sacrificed at indicated time points when peripheral blood and bone marrow from femurs and tibias were collected from each animal.

### CFU in culture assay

Marrow cells were harvested from NSG or C57BL/6 mice as described previously (*36*). Briefly, bone marrow was flushed from femurs and tibias using Iscove's modified Dulbecco's medium (IMDM). Progenitor c-$KIT^+$ cells were then isolated using EasySep Mouse PE Selection Kit (STEMCELL Technologies) following the protocol described by the manufacturer. Murine c-$KIT^+$ cells were cultured in IMDM with 10% vesicle-free FBS and supplements of mouse IL-3 and SCF (50 ng/ml) (R&D Systems). About $1 \times 10^6$ cells were incubated with exosomes harvested from $60 \times 10^6$ to $70 \times 10^6$ HL-60 cells for 48 hours. IMDM was used as the control. Mouse Methylcellulose Complete Media (R&D Systems) were used for CFU assays. The plating concentration was 5000 treated c-$KIT^+$ cells per 35-mm dish. Cells were incubated for 7 days at 37°C with 5% $CO_2$ and ≥95% humidity. Colonies were determined by light microscopy based on morphology and counted at day 7, and the results were averaged from triplicate plates per condition.

### Quantitative RT-PCR

RNA was extracted from exosomes and cells using miRNeasy or RNeasy kits and quantified using a NanoDrop 2000c spectrophotometer (Thermo

Scientific). RNAs were converted into complementary DNA using the SuperScript III First-Strand Synthesis kit (Invitrogen) with oligo(dT) priming, followed by RT-PCR analysis using SYBR Green PCR kit (Applied Biosystems). Sequences of the primers used are listed in table S2. Relative quantification was calculated using the $\Delta\Delta C_T$ algorithm with *Gapdh* as the endogenous control. For miRNA quantification, TaqMan assay kits (Applied Biosystems) were used for reverse transcription and qRT-PCR, using U6 snRNA as the endogenous control.

### Microarray

Microarray assays were performed in the Oregon Health & Science University Gene Profiling Shared Resource facility. For sample quality assessment, RNA quantity and purity were measured by ultraviolet absorbance on the NanoDrop 1000 spectrometer (Thermo Scientific). RNA integrity and size distribution were determined by running each sample on an RNA 6000 Nano chip and a Small RNA chip (Agilent Technologies). For target labeling, total RNA (130 ng) was prepared for hybridization using the FlashTag Biotin HSR miRNA Labeling Kit (Affymetrix) following the manufacturer's recommendations. For array hybridization and processing, hybridization solutions were prepared according to Affymetrix recommendations and injected into a GeneChip miRNA 3.0 Array cartridge (Affymetrix), followed by incubation at 48°C for 18 hours. Arrays were processed according to Affymetrix recommendations and scanned on GeneChip Scanner 3000 7G with autoloader (Affymetrix). Image processing was performed using Affymetrix GeneChip Command Console software, followed by array analysis in Expression Console (Affymetrix), to evaluate array performance and general data quality. All arrays passed performance quality thresholds in the core lab heat map generated using Partek Genomics Suite. Principal components analysis was performed using R.

### Validation of miRNA targets

The 3′UTR of each target was PCR-amplified from HEK293T or primary murine c-KIT$^+$ genomic DNA and cloned into psiCHECK-2 vector (Promega). psiCHECK-2 vector (100 ng) and microRNA mimic (2 nM) (Dharmacon) were cotransfected into $4 \times 10^5$ HEK293 cells that were seeded in a 12-well dish. Cells were washed in PBS 48 hours after transfection and lysed according to the manufacturer's protocol for Dual-Luciferase (Promega). Firefly and Renilla luminescence were measured with Berthold Centro XS$^3$ LB 960 Luminometer, and relative luminescence was compared to relative luminescence of psiCHECK-2 construct transfected without mimic to generate percent knockdown. The negative control miR-6 was a mimic derived from *C. elegans*, which does not bind to mammalian transcripts. Technical triplicates were performed for each biological replicate. Error bars represent the SEM from at least three biological replicates.

### siRNA knockdown of c-Myb

c-KIT$^+$ cells were enriched as described above. Immediately after enrichment, $5 \times 10^4$ cells were electroporated using an Amaxa 4D-Nucleofector X system (Lonza) following the manufacturer's guidelines for CD34$^+$ cells. The transfection used an optimized setting determined by pilot electroporation with a GFP-expressing vector. The siRNA used (OriGene) included two siRNAs targeting *c-Myb* and a negative control siRNA (catalog number SR418501), which was used as the comparative control. A final concentration of 20 nM siRNA was electroporated into cells, and transfection efficiency was compared to cells electroporated with a GFP-expressing vector in parallel. Forty-eight hours after electroporation, 5000 cells were plated in methylcellulose and CFUs were determined as described above.

### shRNA knockdown of miR-155

The miR-Zip miR-155 targeting plasmid was purchased from System Biosciences. Lentiviral particles were produced in HEK293T cells, and successfully transduced HL-60 cells were selected for GFP$^+$ expression by fluorescence-activated cell sorting. miR-155 knockdown was determined by qRT-PCR using RNA extracted with the miRNeasy kit (Qiagen) from cells and from exosome preparations. Cell growth and viability were determined by trypan blue at the time of exosome harvest. Exosome size distribution was determined by nanoparticle tracking analysis using a NanoSight LM10 instrument (Malvern). Protein–to–nucleic acid ratio of exosome preps was determined using a Virus Counter 3100 instrument (ViroCyt).

### Western blot

Western blots were performed as described in (*29*), using GAPDH (Novus Biologicals), p53 (Cell Signaling Technology), and phospho-Ser$^{20}$ p53 antibody (Cell Signaling Technology).

### Anti-miR electroporation

A final concentration of 20 nM anti-miR (Ambion) was electroporated into c-KIT$^+$ cells as described above. Cells recovered in IMDM with 10% vesicle-free FBS and supplements of mouse IL-3 and SCF (50 ng/ml) (R&D Systems) for 2 hours. Cells were then exposed to either HL-60 exosomes or vehicle. Forty-eight hours later, 5000 cells were plated in methylcellulose and CFUs were determined as described above (assay IDs: anti–miR-155, MH12601; anti–miR-150, MH10070; catalog number: anti-miR control, 4464076).

### RISC-trap

RISC-trap experiments of miR-155, miR-137, and miR-132 and data analyses were performed as previously described (*18*), except that reads for each gene were counted by HTSeq (*37*). The cutoffs for determining the final list of miR-155 targets were as follows: fold change ≥ 2 and FDR ≤ 15%. The heat map was plotted using gplots, an R package.

### Statistical analysis

The results are presented as means ± SEM. Student's *t* test was used for comparison between samples derived from the same source (cell or exosome) but subjected to different conditions. For comparisons between parental cell and exosomes, the paired *t* test was conducted to correct for sample relatedness. Unadjusted statistical significance was set at $P \leq 0.05$ followed by implementation of an FDR at $P \leq 0.10$ to correct for multiple testing where relevant.

## SUPPLEMENTARY MATERIALS

www.sciencesignaling.org/cgi/content/full/9/444/ra88/DC1
Fig. S1. In vivo imaging correlates with chimerism.
Fig. S2. Intrafemoral injections of exosomes decrease expression of hematopoietic genes.
Fig. S3. Intravenous injections of exosomes decrease expression of hematopoietic genes.
Fig. S4. miR-155 knockdown in HL-60 cells shows no decrease in viability or proliferation.
Fig. S5. Exosome size profile is unaltered in miR-155 knockdown HL-60 cells.
Table S1. The top transcripts identified by the miR-155 RISC-trap assay.
Table S2. Primer sequences.

## REFERENCES AND NOTES

1. T. Lehrnbecher, L. Sung, Anti-infective prophylaxis in pediatric patients with acute myeloid leukemia. *Expert Rev. Hematol.* **7**, 819–830 (2014).
2. B. Lowenberg, J. R. Downing, A. Burnett, Acute myeloid leukemia. *N. Engl. J. Med.* **341**, 1051–1062 (1999).
3. B. Zhang, Y. W. Ho, Q. Huang, T. Maeda, A. Lin, S.-u. Lee, A. Hair, T. L. Holyoake, C. Huettner, R. Bhatia, Altered microenvironmental regulation of leukemic and normal stem cells in chronic myelogenous leukemia. *Cancer Cell* **21**, 577–592 (2012).

4. K. Schepers, E. M. Pietras, D. Reynaud, J. Flach, M. Binnewies, T. Garg, A. J. Wagers, E. C. Hsiao, E. Passegué, Myeloproliferative neoplasia remodels the endosteal bone marrow niche into a self-reinforcing leukemic niche. *Cell Stem Cell* **13**, 285–299 (2013).
5. F. Miraki-Moud, F. Anjos-Afonso, K. A. Hodby, E. Griessinger, G. Rosignoli, D. Lillington, L. Jia, J. K. Davies, J. Cavenagh, M. Smith, H. Oakervee, S. Agrawal, J. G. Gribben, D. Bonnet, D. C. Taussig, Acute myeloid leukemia does not deplete normal hematopoietic stem cells but induces cytopenias by impeding their differentiation. *Proc. Natl. Acad. Sci. U.S.A.* **110**, 13576–13581 (2013).
6. J. Huan, N. I. Hornick, N. A. Goloviznina, A. N. Kamimae-Lanning, L. L. David, P. A. Wilmarth, T. Mori, J. R. Chevillet, A. Narla, C. T. Roberts, M. M. Loriaux, B. H. Chang, P. Kurre, Coordinate regulation of residual bone marrow function by paracrine trafficking of AML exosomes. *Leukemia* **29**, 2285–2295 (2015).
7. H. Valadi, K. Ekström, A. Bossios, M. Sjöstrand, J. J. Lee, J. O. Lötvall, Exosome-mediated transfer of mRNAs and microRNAs is a novel mechanism of genetic exchange between cells. *Nat. Cell Biol.* **9**, 654–659 (2007).
8. Y. Chen, R. Jacamo, M. Konopleva, R. Garzon, C. Croce, M. Andreeff, CXCR4 down-regulation of let-7a drives chemoresistance in acute myeloid leukemia. *J. Clin. Invest.* **123**, 2395–2407 (2013).
9. A. A. Wilson, L. W. Kwok, E. L. Porter, J. G. Payne, G. S. McElroy, S. J. Ohle, S. R. Greenhill, M. T. Blahna, K. Yamamoto, J. C. Jean, J. P. Mizgerd, D. N. Kotton, Lentiviral delivery of RNAi for in vivo lineage-specific modulation of gene expression in mouse lung macrophages. *Mol. Ther.* **21**, 825–833 (2013).
10. M. D. Muzumdar, B. Tasic, K. Miyamichi, L. Li, L. Luo, A global double-fluorescent Cre reporter mouse. *Genesis* **45**, 593–605 (2007).
11. N. I. Hornick, J. Huan, B. Doron, N. A. Goloviznina, J. Lapidus, B. H. Chang, P. Kurre, Serum exosome microRNA as a minimally-invasive early biomarker of AML. *Sci. Rep.* **5**, 11295 (2015).
12. Q. Yin, J. McBride, C. Fewell, M. Lacey, X. Wang, Z. Lin, J. Cameron, E. K. Flemington, MicroRNA-155 is an Epstein-Barr virus-induced gene that modulates Epstein-Barr virus-regulated gene expression pathways. *J. Virol.* **82**, 5295–5306 (2008).
13. B. Muylkens, D. Coupeau, G. Dambrine, S. Trapp, D. Rasschaert, Marek's disease virus microRNA designated Mdv1-pre-miR-M4 targets both cellular and viral genes. *Arch. Virol.* **155**, 1823–1837 (2010).
14. H. Sakamoto, G. Dai, K. Tsujino, K. Hashimoto, X. Huang, T. Fujimoto, M. Mucenski, J. Frampton, M. Ogawa, Proper levels of c-Myb are discretely defined at distinct steps of hematopoietic cell development. *Blood* **108**, 896–903 (2006).
15. Y. Zhang, H. Jin, L. Li, F. X.-F. Qin, Z. Wen, cMyb regulates hematopoietic stem/progenitor cell mobilization during zebrafish hematopoiesis. *Blood* **118**, 4093–4101 (2011).
16. R. Su, H.-S. Lin, X.-H. Zhang, X.-L. Yin, H.-M. Ning, B. Liu, P.-F. Zhai, J.-N. Gong, C. Shen, L. Song, J. Chen, F. Wang, H.-L. Zhao, Y.-N. Ma, J. Yu, J.-W. Zhang, MiR-181 family: Regulators of myeloid differentiation and acute myeloid leukemia as well as potential therapeutic targets. *Oncogene* **34**, 3226–3239 (2015).
17. K. A. Lennox, M. A. Behlke, Chemical modification and design of anti-miRNA oligonucleotides. *Gene Ther.* **18**, 1111–1120 (2011).
18. X. A. Cambronne, R. Shen, P. L. Auer, R. H. Goodman, Capturing microRNA targets using an RNA-induced silencing complex (RISC)-trap approach. *Proc. Natl. Acad. Sci. U.S.A.* **109**, 20473–20478 (2012).
19. H. Dweep, N. Gretz, C. Sticht, miRWalk database for miRNA-target interactions. *Methods Mol. Biol.* **1182**, 289–305 (2014).
20. A. Franceschini, D. Szklarczyk, S. Frankild, M. Kuhn, M. Simonovic, A. Roth, J. Lin, P. Minguez, P. Bork, C. von Mering, L. J. Jensen, STRING v9.1: Protein-protein interaction networks, with increased coverage and integration. *Nucleic Acids Res.* **41**, D808–D815 (2013).
21. P. Shannon, A. Markiel, O. Ozier, N. S. Baliga, J. T. Wang, D. Ramage, N. Amin, B. Schwikowski, T. Ideker, Cytoscape: A software environment for integrated models of biomolecular interaction networks. *Genome Res.* **13**, 2498–2504 (2003).
22. E. M. Pinto, R. C. Ribeiro, B. C. Figueiredo, G. P. Zambetti, TP53-associated pediatric malignancies. *Genes Cancer* **2**, 485–490 (2011).
23. T. S. Elton, H. Selemon, S. M. Elton, N. L. Parinandi, Regulation of the MIR155 host gene in physiological and pathological processes. *Gene* **532**, 1–12 (2013).
24. M. D. Delgado, M. Albajar, M. T. Gomez-Casares, A. Batlle, J. Léon, MYC oncogene in myeloid neoplasias. *Clin. Transl. Oncol.* **15**, 87–94 (2013).
25. E. L. Artinger, B. P. Mishra, K. M. Zaffuto, B. E. Li, E. K. Y. Chung, A. W. Moore, Y. Chen, C. Cheng, P. Ernst, An MLL-dependent network sustains hematopoiesis. *Proc. Natl. Acad. Sci. U.S.A.* **110**, 12000–12005 (2013).
26. C. P. Koh, C. Q. Wang, C. E. L. Ng, Y. Ito, M. Araki, V. Tergaonkar, G. Huang, M. Osato, RUNX1 meets MLL: Epigenetic regulation of hematopoiesis by two leukemia genes. *Leukemia* **27**, 1793–1802 (2013).
27. M. Scheller, J. Huelsken, F. Rosenbauer, M. M. Taketo, W. Birchmeier, D. G. Tenen, A. Leutz, Hematopoietic stem cell and multilineage defects generated by constitutive β-catenin activation. *Nat. Immunol.* **7**, 1037–1047 (2006).
28. Y.-H. Ou, P.-H. Chung, T.-P. Sun, S.-Y. Shieh, p53 C-terminal phosphorylation by CHK1 and CHK2 participates in the regulation of DNA-damage-induced C-terminal acetylation. *Mol. Biol. Cell* **16**, 1684–1695 (2005).
29. J. Huan, N. I. Hornick, M. J. Shurtleff, A. M. Skinner, N. A. Goloviznina, C. T. Roberts, P. Kurre, RNA trafficking by acute myelogenous leukemia exosomes. *Cancer Res.* **73**, 918–929 (2013).
30. B. Xia, C. Tian, S. Guo, L. Zhang, D. Zhao, F. Qu, W. Zhao, Y. Wang, X. Wu, W. Da, S. Wei, Y. Zhang, c-Myc plays part in drug resistance mediated by bone marrow stromal cells in acute myeloid leukemia. *Leuk. Res.* **39**, 92–99 (2015).
31. B. Pezeshkian, C. Donnelly, K. Tamburo, T. Geddes, G. J. Madlambayan, Leukemia mediated endothelial cell activation modulates leukemia cell susceptibility to chemotherapy through a positive feedback loop mechanism. *PLOS One* **8**, e60823 (2013).
32. P. Chandran, Y. Le, Y. Li, M. Sabloff, J. Mehic, M. Rosu-Myles, D. S. Allan, Mesenchymal stromal cells from patients with acute myeloid leukemia have altered capacity to expand differentiated hematopoietic progenitors. *Leuk. Res.* **39**, 486–493 (2015).
33. S. A. Melo, H. Sugimoto, J. T. O'Connell, N. Kato, A. Villanueva, A. Vidal, L. Qiu, E. Vitkin, L. T. Perelman, C. A. Melo, A. Lucci, C. Ivan, G. A. Calin, R. Kalluri, Cancer exosomes perform cell-independent microRNA biogenesis and promote tumorigenesis. *Cancer Cell* **26**, 707–721 (2014).
34. J. R. White, K. Weston, Myb is required for self-renewal in a model system of early hematopoiesis. *Oncogene* **19**, 1196–1205 (2000).
35. Z. He, J. Cai, J.-W. Lim, K. Kroll, L. Ma, A novel KRAB domain-containing zinc finger transcription factor ZNF431 directly represses *Patched1* transcription. *J. Biol. Chem.* **286**, 7279–7289 (2011).
36. A. M. Skinner, M. Grompe, P. Kurre, Intra-hematopoietic cell fusion as a source of somatic variation in the hematopoietic system. *J. Cell Sci.* **125**, 2837–2843 (2012).
37. S. Anders, P. T. Pyl, W. Huber, HTSeq—A Python framework to work with high-throughput sequencing data. *Bioinformatics* **31**, 166–169 (2015).


**Acknowledgments:** We acknowledge assistance by M. Fisher for the Gene Expression Omnibus data set submission. **Funding:** This study was supported by the Hyundai Hope on Wheels Foundation (to P.K.) and NIH/National Institute of Allergy and Infectious Diseases grant 5T32AI78903-5 (to N.I.H). **Author contributions:** N.I.H. conceptualized and performed experiments, analyzed the data, and wrote the manuscript; B.D. conceptualized and performed experiments, analyzed the data, and wrote the manuscript; S.A. performed experiments and analyzed the data; J.H. performed experiments and analyzed the data; C.A.H. performed experiments and analyzed the data; R.S. analyzed the data; X.A.C. performed experiments; S.C.V. conceptualized and performed experiments and analyzed the data; P.K. conceptualized experiments, analyzed the data, and wrote the manuscript. **Competing interests:** X.A.C. was involved in the commercial licensing of the RISC-trap technology. This did not influence the experimental design, data collection, or analysis of the project data. **Data and materials availability:** Array data are deposited to National Center for Biotechnology Information (http://ncbi.nlm.nih.gov/geo/query/acc.cgi?acc=GSE85769), accession ID GSE85769.

Submitted 20 January 2016
Accepted 18 August 2016
Final Publication 6 September 2016
10.1126/scisignal.aaf2797
**Citation:** N. I. Hornick, B. Doron, S. Abdelhamed, J. Huan, C. A. Harrington, R. Shen, X. A. Cambronne, S. Chakkaramakkil Verghese, P. Kurre, AML suppresses hematopoiesis by releasing exosomes that contain microRNAs targeting c-MYB. *Sci. Signal.* **9**, ra88 (2016).

# AML suppresses hematopoiesis by releasing exosomes that contain microRNAs targeting c-MYB

Noah I. Hornick, Ben Doron, Sherif Abdelhamed, Jianya Huan, Christina A. Harrington, Rongkun Shen, Xiaolu A. Cambronne, Santhosh Chakkaramakkil Verghese and Peter Kurre

*Sci. Signal.* **9** (444), ra88.
DOI: 10.1126/scisignal.aaf2797

**AML dispatches micromanagers**

In patients with acute myeloid leukemia (AML), the production of healthy blood cells from hematopoietic stem cells in the bone marrow (a process called hematopoiesis) is suppressed, prompting the need for bone marrow transplants. AML cells shed extracellular vesicles called exosomes that contain molecules that suppress hematopoiesis by reprogramming the stem cell niche. Hornick *et al*. discovered another way that AML exosomes block this critical process by delivering microRNAs to hematopoietic stem cells. The AML-derived exosomes contained two mature microRNAs that target the mRNA encoding c-MYB, a transcription factor involved in hematopoiesis. Other targets of these AML-derived exosomal microRNAs reveal interconnected networks targeting transcripts that produce proteins that control the cell cycle. The findings suggest that disrupting this mode of intercellular communication might enhance hematopoiesis in AML patients.